Resolved Conformational States of Spin-Labeled Ca-ATPase during the Enzymatic Cycle†

Scott M. Lewis and David D. Thomas*

Department of Biochemistry, University of Minnesota Medical School, Minneapolis, Minnesota 55455

Received April 8, 1992; Revised Manuscript Received May 22, 1992

ABSTRACT: We have used frequency- and time-resolved electron paramagnetic resonance (EPR) to study the effects of substrate on the nanosecond conformational dynamics of the Ca-ATPase of sarcoplasmic reticulum, as detected by an iodoacetamide spin label (IASL) attached covalently to the enzyme. We confirm previous results [Coan, C. (1983) *Biochemistry 22*, 5826] showing that this probe is less rotationally mobile following the addition of nucleotides (ADP, AMPPNP, ATP) and that the shape of the spectrum suggests the presence of two components. We used two approaches to enhance EPR resolution in order to resolve the spectral components and their corresponding conformational states. First, to improve resolution in the *frequency (spectral) domain*, we used perdeuterated IASL, which results in narrower line widths. Digital spectral analysis resolves the EPR spectrum into two components, one that is indistinguishable from the spectrum observed in the absence of ligands and another that indicates more restricted probe motions, suggesting a distinct conformation of the labeled protein. Additions of substrate ligands appear to change only the mole fractions of the two components. The mole fraction of the restricted component (f_R) was 0 in the absence of ligands, but increased to about 0.5 in the presence of saturating concentrations of AMPPNP and Ca^{2+}. In general, ATP and its analogs increase f_R, with larger effects observed in the presence of Ca. However, calcium has no effect by itself ($f_R = 0$). Both monovanadate and decavanadate increase f_R, but the formation of a covalent phosphoenzyme from inorganic phosphate (E_2-P) had no effect ($f_R = 0$). Thus, although these EPR spectra are sensitive to conformational transitions in the Ca-ATPase, these transitions are not consistent with a simple E_1–E_2 conformational model, which predicts that the addition of calcium (to form Ca_2·E1) should induce a conformation different from that induced by inorganic phosphate (to form E_2-P). Our second means of resolution enhancement was in the *time domain*. In order to detect transients in the restricted fraction during Ca-ATPase activity, we used a laser pulse to photolyze caged ATP during EPR data acquisition. We observed a rapid increase in f_R, followed by partial recovery to an intermediate steady-state level, indicating pre-steady-state conformational changes in the transport cycle. We conclude that the Ca-ATPase can exist in at least two conformations, which are distinguishable on the basis of internal protein dynamics, and whose relative populations are dependent on ligands during the active transport cycle.

The sarcoplasmic reticulum (SR[1]) Ca-ATPase is responsible for active calcium transport in skeletal muscle. A widely proposed enzyme cycle (Scheme I) involves two basic enzyme conformations, E_1 and E_2, which play a central role in coupling ATP hydrolysis to Ca^{2+} transport. However, studies have suggested conformational transitions in addition to these two states that occur at key steps in the cycle, including calcium binding to the high-affinity sites, ATP binding, phosphoenzyme formation, calcium translocation and release, and phosphoenzyme decomposition [reviewed by Jencks (1989) and Inesi et al. (1990)].

In the absence of substrates, the resting enzyme is proposed to exist as an equilibrium mixture of E_1 and E_2, with E_1 being favored by micromolar Ca^{2+}, high pH, and low temperature (Sumida et al., 1978; Pick & Karlish, 1982). This proposed conformational change due to calcium binding is supported by calcium-induced changes in intrinsic tryptophan fluorescence (Dupont & Leigh, 1978; Ikemoto et al., 1978; Pick & Karlish, 1980), sulfhydryl reactivity (Murphy, 1978), fluorescence of a bound fluorescent dye (Yasuoka-Yabe & Kawakita, 1983), Fourier-transform infrared spectroscopy (Arrondo et al., 1987), and circular dichroism (Girardet & Dupont, 1992).

Scheme I: Proposed Ca-ATPase Kinetic Cycle

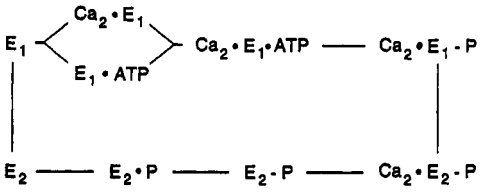

With the addition of ATP (or an ATP analog), the Ca_2·E_1·nucleotide state is formed. For ATP this leads to the phosphorylated enzyme, Ca_2·E_1-P. On the basis of kinetic studies, Petithory and Jencks (1986) proposed an ATP-induced conformational transition. Using EPR spectroscopy on a piperidinyliodoacetamide spin label (IASL) attached to the Ca-ATPase, Coan and Inesi (1977) noted that ATP and calcium

† This work was supported by a grant to D.D.T. from the National Institutes of Health (AR39754). S.M.L. was supported by a scholarship from the Life & Health Insurance Medical Research Fund.

[1] Abbreviations: SR, sarcoplasmic reticulum; DOCSR, deoxycholic acid treated sarcoplasmic reticulum; EPR, electron paramagnetic resonance; MSL, *N*-(1-oxy-2,2,6,6-tetramethyl-4-piperidinyl)maleimide; IASL, *N*-(1-oxy-2,2,6,6-tetramethyl-4-piperidinyl)iodoacetamide; NEM, *N*-ethylmaleimide; SRB, sarcoplasmic reticulum buffer; V_i, vanadate; EGTA, ethylene glycol bis(β-aminoethyl ether)-*N*,*N*,*N*′,*N*′-tetraacetic acid; DMF, dimethylformamide; DMSO, dimethyl sulfoxide; P_i, inorganic phosphate; AMPPNP, β,δ-imidoadenosine 5′-triphosphate; caged ATP, adenosine 5′-triphosphate, P^3-1-(2-nitrophenyl)ethyl ester; MOPS, 3-(*N*-morpholino)propanesulfonic acid; MES, 2-(*N*-morpholino)ethanesulfonic acid; IAEDANS, 5-[2-[(iodoacetyl)amino]ethyl]aminonaphthalene-1-sulfonic acid.

0006-2960/92/0431-7381$03.00/0

broadened the spectrum, indicating restricted mobility in the spin-labeled protein. These studies were extended to other ligands, including AMPPNP and ADP (Coan et al., 1979; Coan & Keating, 1982; Coan, 1983). Using fluorescence spectroscopy to study an IAEDANS-labeled Ca-ATPase, Kubo et al. (1990) reported that nucleotides, acetyl phosphate, and carbamyl phosphate induced an increase in probe mobility that was enhanced by calcium. Similar results were reported by Laggner et al. (1981) using a pyrrolidinyliodoacetamide spin label.

The presumed calcium translocation step, Ca_2-E_1-P to Ca_2-E_2-P, involves another proposed conformational change (Brandl et al., 1986). Following ATP-induced phosphorylation and calcium translocation, differences were reported in sulfhydryl reactivity (Murphy, 1978), X-ray diffraction (Blasie et al., 1990), and the emission of attached fluorescent probes (Watanabe & Inesi, 1982b; Suzuki et al., 1987). Using the inhibitor Cr-ATP, Vilsen and Andersen (1987) observed different triptic cleavage patterns upon calcium occlusion. A nonutilizable form of ADP was reported to promote a conformational change in the phosphorylated enzyme, presumably Ca_2-E_1-P (Yasuoka-Yabe et al., 1983).

It is proposed that E_2-P is formed following calcium release. This state can be obtained by addition of inorganic phosphate under the appropriate conditions (low pH, no potassium, low magnesium, presence of DMSO). Formation of this intermediate changes the circular dichroism of the Ca-ATPase, suggesting changes in secondary structure (Girardet & Dupont, 1992). Studies using light scattering and fluorescence energy transfer (Watanabe & Inesi, 1982a) and EPR spectroscopy (Coan, 1983) suggested a conformational transition upon phosphoenzyme formation by both ATP and inorganic phosphate. A conformational transition was also suggested by the effect of vanadate, a Ca-ATPase inhibitor that presumably acts by binding in place of inorganic phosphate and mimicking the E_2-P state. Vanadate binding alters triptic susceptibility of the Ca-ATPase (Dux & Martonosi, 1983b) and induces broadening of the EPR system of an IASL-labeled Ca-ATPase (Coan et al., 1986).

In summary, a large number of studies have documented ligand-induced structural and mobility changes in the Ca-ATPase. However, none of these studies has resolved and quantitated discrete protein conformations induced by ligands in the Ca-ATPase cycle. It is important to know whether there is a physical basis for the proposed E_1 and E_2 conformational states, and whether transitions between other distinct conformations occur in the reaction cycle. Conformational changes can affect segmental (nanosecond) as well as global (microsecond) protein mobility. Previous studies using saturation-transfer EPR, which is sensitive to global, microsecond motions and protein–protein interactions in the Ca-ATPase (Lewis & Thomas, 1986; Squier & Thomas, 1988) found no changes due to ATPase ligands (Lewis & Thomas, 1991), implying no significant change in the oligomeric state or hydrodynamic shape of the enzyme. Therefore, if conformational changes occur, they may only affect *internal* structure and dynamics, as detected optimally by conventional EPR.

Therefore, the goal of the present study is to resolve and quantitate the conformational components suggested by previous conventional EPR studies on iodoacetamide-spin-labeled SR (Coan, 1983; Coan et al., 1986). We have studied the effects of ligands on these components, providing insight into possible reaction intermediates. To maximize our ability to resolve these conformational transitions, we have used two approaches. *Enhanced resolution in the frequency domain* was obtained by using perdeuterated spin labels, which have narrower intrinsic line widths and thus improved spectral resolution (Fajer et al., 1990). Finally, we have obtained *time resolution* during the ATPase reaction cycle by using laser-pulse-induced photolysis of caged ATP during EPR data acquisition.

METHODS

Preparation of Membrane Vesicles. Sarcoplasmic reticulum (SR) vesicles were prepared from the white (fast) skeletal muscle of New Zealand white rabbits according to the method of Fernandez et al. (1980). The SR was suspended in sucrose buffer (0.3 M sucrose, 20 mM MOPS, pH 7.0) at a concentration of 20–40 mg/mL, rapidly frozen, and stored in liquid nitrogen until use. DOCSR vesicles were produced by treating SR vesicles with deoxycholic acid (DOC) according to Hildago et al. (1978) and Squier and Thomas (1988). Protein concentrations were determined by the biuret assay, using bovine serum albumin as a standard (Gornall et al., 1949).

Fractionation of the SR Preparation. The SR preparation was layered on a discontinuous sucrose gradient (25/35/40/50) and centrifuged 12 h at 85000*g*. The fractions taken were as follows: surface membranes, 25%/35% interface; light SR, 35%/40% interface; intermediate SR, 40% layer; heavy SR, 40%/50% interface. The samples were washed in sucrose buffer as above. The percentages (by weight of protein) of these fractions were 4.3 ± 1.7% surface membranes, 13.6 ± 3.1% light SR, 30.9 ± 0.8% intermediate SR, and 51.3 ± 5.6% heavy SR, in good agreement with previous results (Fernandez et al., 1980).

Solutions. All experiments were performed in 0.1 M KCl, 10 mM imidazole, 0.5 mM EGTA, 5 mM $MgCl_2$, pH 7.4 (Dux & Martonosi, 1983a), designated SR buffer (SRB) unless otherwise specified. All vanadate solutions were made from Na_3VO_4 obtained from Fischer Scientific Co. Stock solutions of monovanadate and decavanadate were prepared according to Dux and Martonosi (1983a) and Varga et al. (1985) and characterized according to Lewis and Thomas (1986). In the discussions that follow, vanadate concentrations are given in terms of the total moles of vanadium present without correction for polymerization. AMPPNP was obtained from Sigma Chemicals. A23187 (Calbiochem) solutions were made in dimethylformamide (DMF) and stored at −20 °C until use. Caged ATP (obtained from Dr. Yale Goldman), IASL (obtained from Aldrich Chemicals), and perdeuterated IASL solutions (obtained from Dr. A. H. Beth) were stored in the dark in liquid nitrogen until use. Concentrated spin label stock solutions were in DMF.

ATP Hydrolysis Activity. ATPase activities were measured by determining the rate of steady-state phosphate liberation in the presence of 5 mM MgATP, using an assay for inorganic phosphate essentially as described by Lanzetta et al. (1977). Activity was measured with and without calcium. The protein concentration was 0.05 mg/mL unless otherwise specified. The amount of added ionophore, A23187, was calibrated for each preparation of SR in order to ensure full activation of activity. This was typically 1 μg/0.05 mg of SR protein. The reaction was started by the addition of 5 mM ATP.

Calcium Uptake Activity. Calcium uptake activity was assayed in a buffer containing 0.025 mg/mL SR protein, 0.1 M KCl, 5 mM $MgCl_2$, 5 mM potassium oxalate, 20 mM MOPS, pH 7.0, 0.1 mM $CaCl_2$, and 1 μCi of $^{45}CaCl_2$. The reaction was started by the addition of 4 mM ATP. Sequential aliquots were filtered through 0.45-μm Millipore filters. The

filtrates were counted in a scintillation counter with all channels open. The zero time point was subtracted from the subsequent values. These were then related to accumulated calcium by counting a sample of the unfiltered reaction mixture. The activity was taken from the initial slope of a plot of moles of Ca taken up per milligram of SR protein versus time.

Phosphoenzyme Formation. The phosphoenzyme formed from inorganic phosphate was assayed essentially according to the procedure of Barrabin et al. (1984), as described in detail by Lewis and Thomas (1991). The $H_3{}^{32}PO_4$ was obtained from New England Nuclear. The assay tubes contained 100 μg of SR protein in the phosphorylation buffer (variable). Inorganic phosphate (containing ^{32}P) was added to produce a concentration of 5 mM. Phosphoenzyme was quantitated by dividing moles of P_i bound by moles of Ca-ATPase (taking into account the percentage of the SR protein, determined by gel electrophoresis, that is the Ca-ATPase).

Lipid-to-Protein Ratio. The lipid-to-protein ratio was calculated as the moles of phospholipid divided by the moles of Ca-ATPase [calculated by multiplying the protein concentration by the fraction of Ca-ATPase present (determined by gel electrophoresis) and dividing by a molecular mass of 115 kDa]. The phospholipid concentration was determined by the method of Chen et al. (1956). The ratio of SR preparations was 75 ± 5% and for DOCSR preparations was 85 ± 10%.

Protein Labeling. Labeling stoichiometry was defined as the number of labels per Ca-ATPase. The concentration of label was determined by comparing the double integral of the EPR spectrum to the double integral of the spectrum for a 0.5 mM solution of the free label. This was then divided by the Ca-ATPase concentration in molar units.

The labeling conditions were derived from several experiments which are described in detail in Results. The final protocol is as follows. The Ca-ATPase was prelabeled with *N*-ethylmaleimide (NEM) for 30 min at 25 °C in sucrose buffer. The Ca-ATPase concentration was 10 mg/mL SR protein, and the NEM concentration was 0.10 mM. This was followed by the addition of 2 mol of IASL/mol of Ca-ATPase, corresponding to a concentration of 0.20 mM IASL. After a 3-h incubation at 25 °C, the sample was diluted in cold sucrose buffer, centrifuged at 100000*g*, and resuspended in SRB buffer minus EGTA. The sample was again centrifuged and then resuspended in the experimental buffer. The final stoichiometry was 0.52 ± 0.01 IASL/Ca-ATPase.

EPR Sample Preparation. Samples were suspended in the appropriate buffer by centrifuging in SRB minus EGTA for 45 min at 100000*g*. The pellets were resuspended in the experimental buffer. Ligand additions were made to the resuspended sample. Twenty-four-hour vanadate samples were prepared by incubation of 30–40 mg/mL protein with 5 mM mono- or decavanadate for 1 day at pH 7.4 in SRB at 4 °C. To ensure saturating concentrations of calcium and AMPPNP, the spectral changes were titrated. AMPPNP in 5 and 10 mM concentrations gave the identical spectral parameters and fractions. AMPPNP at 2.5 mM resulted in smaller values. Calcium was found to be saturating at all concentrations used in these experiments (micromolar to millimolar). In order to ensure that the ligand additions were not affecting the pH of the buffer, identical experiments were done in SRB with 40 mM imidazole at pH 7.4. These results obtained were identical to those in SRB with 10 mM imidazole.

EPR Spectral Acquisition. EPR spectra were obtained with a Varian E-109 EPR spectrometer interfaced to a Northstar computer, following the procedures described in detail by Squier and Thomas (1986a,b). Samples were placed in a capillary made from the gas-permeable plastic TPX (Bigelow et al., 1986) and degassed with N_2 for 20 min prior to scanning, since it was previously shown that O_2 affects protein spectra (Squier & Thomas, 1986a). Conventional EPR spectra, which are sensitive to nanosecond motions and are designated V_1, were obtained with 100-kHz field modulation (with a modulation amplitude of 2 G), using a microwave field amplitude (H_1) of 0.14 G for the Ca-ATPase spectra.

EPR Spectra Acquisition for Caged ATP Experiments. These spectra were acquired as above, except that a Bruker ER 200D EPR spectrometer was used and the samples were contained in an optically clear quartz flat cell. The surface of the quartz temperature control dewar was roughed with diamond paste to ensure uniform distribution of light over the sample, as verified with photosensitive film. A Lambda Physik EMG 53 MSC XeCl excimer laser was used to release the ATP (Kaplan et al., 1978; McCray et al., 1980) by directing the beam (308 nm) through radiation slits into the EPR cavity (Bruker TE101). The sample, in a 50-μL quartz flat cell (0.5-mm path length), was positioned in the beam and 20–30% of the 5 mM caged ATP was converted to ATP by a 1-s burst of 50 pulses, each of which had an energy density of about 5 mJ/cm^2. Thermocouple measurements showed that this produced negligible heating, but ATPase measurements before and after the caged ATP photolysis experiment showed that ATPase activity typically dropped by 12%, probably due to reaction of photochemical byproducts with the enzyme (McCray et al., 1980). Thus the inhibition during the brief Ca_2-E_1-P transient was probably less than 12%.

EPR Spectral Analysis. Conventional EPR spectra were characterized by spectral line-height parameters (A/B, C/B) and the maximal field splitting, $2T_{\parallel}'$. A and B are the low-field peak heights; C is the field position of maximal sensitivity to the observed spectral changes [Coan and Inesi, (1977); illustrated in Figure 2 below]. An effective order parameter was calculated from EPR spectral splittings by the method of Squier (1989). The maximal field splittings for the free probe and the fully immobilized probe were used as end points. This order parameter should not be taken to provide an accurate physical description of the probe motion, since spectral splittings can be affected by changes in environmental polarity and motional rate, as well as the motional amplitude, which is the only factor considered in the order parameter calculations.

Spectral Subtraction. Spectral subtractions were done by computer analysis of digitized spectra according to the method of Jost and Griffith (1978). The end-point spectrum was subtracted stepwise from the composite spectrum to obtain the other end point. The choice of end points is discussed in Results.

RESULTS

Labeling the Ca-ATPase with IASL. Initial labeling experiments were performed according to Coan and Inesi (1977). This involved a 1–2-h incubation of the Ca-ATPase vesicles (3 mg/mL) with 0.6–1.2 mM IASL, corresponding to a ratio of about 20–40 labels/Ca-ATPase. This resulted in a spectrum containing at least two components: a primary component with a maximal splitting of 52 G and a minor component (accounting for less than 5% of the spin label) with sharper lines and a splitting of less than 40 G (see Figure 1). The narrower splitting of the latter component implies more nanosecond rotational mobility; such a component is often referred to as "weakly immobilized" (Figure 1, peak *A*),

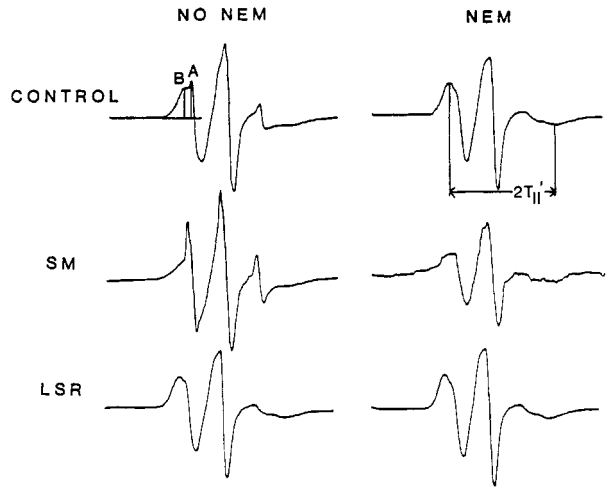

FIGURE 1: EPR spectra of [^{1}H]-IASL attached to the Ca-ATPase in SR vesicles, recorded in sucrose buffer at 4 °C. The labeling stoichiometry was 0.5. The samples in the right column were prelabeled with *N*-ethylmaleimide at a stoichiometry of 1:1. The samples in the left column were not. The middle and bottom rows are two fractions from a sucrose gradient fractionation. Key: control, the starting material before the gradient; SM, surface membranes; LSR, light SR. The spectra of the intermediate SR and heavy SR fractions were similar to those of the light SR fraction. The line-height parameters, *A* and *B*, and the maximal field splitting, $2T_{\parallel}'$, are illustrated.

as compared with the "strongly immobilized" component (Figure 1, peak *B*). The goal in further labeling experiments was to reduce this minor component in order to produce a single-component spectrum that could be easily analyzed.

Three modifications of the labeling protocol lead to a reduction of component *A*. First by use of a labeling at a ratio of 2:1 (10 mg/mL SR protein and 0.20 mM IASL) instead of 20:1, the ratio of *A*/*B* (defined in Figure 1) was decreased. This also resulted in a decrease in the stoichiometry of bound label from 1.1 to 0.7. The second modification was prelabeling the Ca-ATPase with *N*-ethylmaleimide (NEM) at a ratio of 1:1 (10 mg/mL SR protein and 0.10 mM NEM). This approach blocks fast-reacting sulfhydryls in the Ca-ATPase preparation that were responsible for a weakly immobilized component in the MSL–Ca-ATPase spectrum (Thomas & Hidalgo, 1978). In all SR preparations for all labeling stoichiometries, this decreased *A*/*B* with an accompanying 20% decrease in the amount of label bound. Adding more NEM in the prelabeling step did not further decrease the *W* component. The third modification involved labeling a purified Ca-ATPase, namely, DOCSR. In preparations without NEM prelabeling, the ratio of *A*/*B* was lower in the DOCSR sample as compared to the SR sample. However, at 2:1 IASL labeling with a 1:1 NEM prelabel, there was no difference between SR and DOCSR. Since DOCSR preparations contain inverted Ca-ATPase (Herbette et al., 1981), SR was chosen as the Ca-ATPase preparation.

In order to determine the origin of the weakly immobilized component, the labeled SR preparation was fractionated on a discontinuous sucrose gradient. This was done to samples with and without an NEM prelabel (see Figure 1). For the NEM-prelabeled sample the spectral line shape did not change in the various fractions. For the nonprelabeled sample, the weakly immobilized (*A*) component migrated primarily with the surface membranes, suggesting that this component arises from non-Ca-ATPase origins. The presence of some of the strongly immobilized component in the surface membrane fraction is consistent with Ca-ATPase contamination (Fernandez et al., 1980).

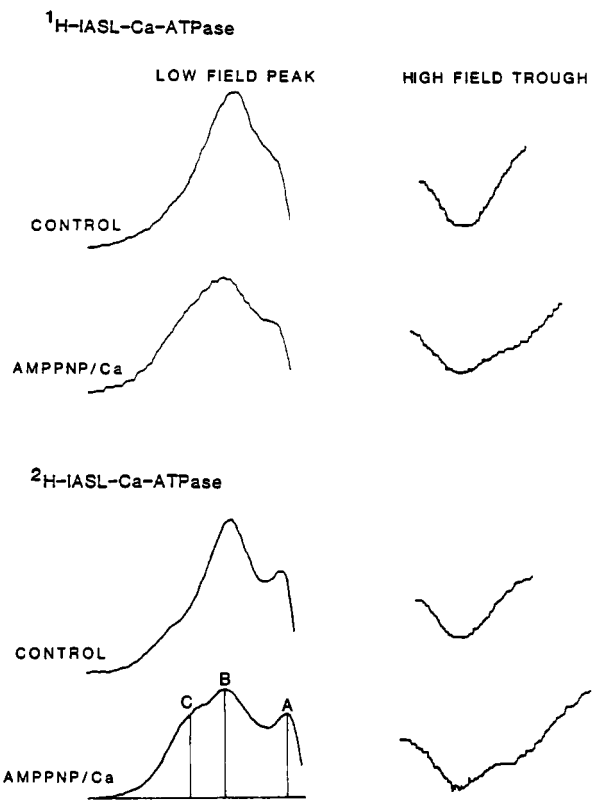

FIGURE 2: EPR spectra of [^{1}H]-IASL–Ca-ATPase and [^{2}H]-IASL–Ca-ATPase, showing the effects of 5 mM AMPPNP and 0.45 mM $CaCl_2$. Spectra were recorded at 4 °C at 20 mg of protein/mL. Stoichiometries for both probes are 0.5. The line-height parameters, *A*, *B*, and *C*, are shown on the AMPPNP/Ca spectrum. The buffer was SRB. The baselines are identical.

The spin label had no effect on the Ca-ATPase activity, measured at 4 and 25 °C. The incubation itself inhibited the ATPase activity, but by less than 20% of the control value. The calcium uptake activity was identical between the labeled and unlabeled control, but again the incubation lowered the activity, presumably by increasing vesicle permeability as suggested by a smaller increase in ATPase activity upon addition of the calcium ionophore A23187.

The final protocol for IASL labeling involves a 1:1 prelabeling with NEM for 30 min at 25 °C in sucrose buffer and 10 mg/mL SR protein. This is followed by the addition of 2 mol of IASL/mol of Ca-ATPase, and an incubation for 3 h at the same temperature (for further details see Methods). The final stoichiometry of bound labels was 0.52 ± 0.01 IASL/Ca-ATPase, 95% of which appears to be a single motional component.

Effect of Ligands on the EPR Line Shape. For improved resolution of spectral components in the ligand studies, a perdeuterated derivative of IASL (referred to as [^{2}H]-IASL) was used. Due to the lack of hyperfine interaction with the neighboring methyl groups, the spectrum has narrower line widths. The deuterated probe resulted in the same labeling stoichiometry as the protonated probe.

Certain ligands produced a broadening of the EPR spectrum. Figure 2 illustrates the difference between [^{1}H]- and [^{2}H]-IASL. The low- and high-field peaks are shown for clarity only. The addition of AMPPNP/Ca broadened the peaks for both probes. However, the spectrum from the deuterated probe showed resolved features. Therefore this probe was used to isolate the restricted component. The two forms of IASL responded similarly to the added ligands. Peak *A*

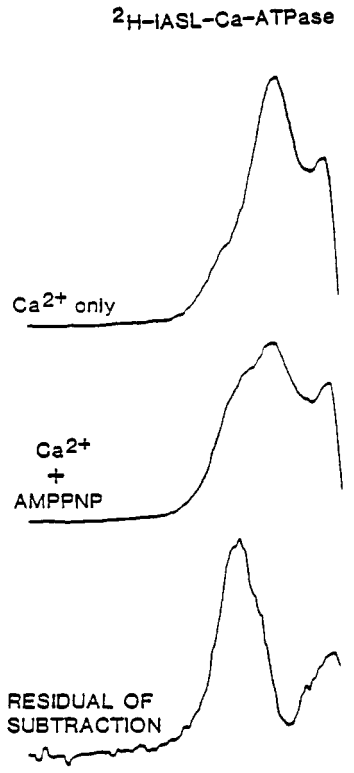

FIGURE 3: Spectral subtractions on [^{2}H]-IASL–Ca-ATPase. Conventional EPR spectra for the control and the AMPPNP/Ca were obtained as in Figure 2. Only the low-field peak is illustrated. Spectra were normalized to the same number of labels prior to plotting. The bottom spectrum was obtained by subtracting the top (control) spectrum from the middle (composite) spectrum (mole fractions are listed in Results).

(weakly immobilized) was not affected by ligand addition except in the case of DMSO.

Spectral Subtractions. In order to isolate the restricted component, spectral subtractions were performed as described in Methods. The control spectrum (without the added ligand) was chosen as one end point (designated the mobile component). The other end point was reached by subtractions and was called the restricted component. The control spectrum was subtracted from the composite spectrum (with the added ligand) in stepwise increments. The end point was reached when the low-field peak was symmetrical, as required by EPR theory (Freed, 1976). This peak was chosen since it clearly demonstrated the restricted component and the asymmetric broadening that resulted from its presence. This portion of the spectrum provided a substantial increase in signal-to-noise ratio over the high-field peak, and the resolution of the two components was much better than in the central peak. In the following ligand studies, a consistent end-point spectrum was reached for all samples. This end-point spectrum was virtually identical for samples containing nucleotides (with and without calcium) and vanadate at pH 7.4. An example is shown in Figure 3 for AMPPNP and calcium. The two end points and composite spectrum are shown. The two end points are characterized by an effective order parameter, S, and the maximal splitting parameter, $2T_{\parallel}'$. For the mobile component, $S = 0.53$ and $2T_{\parallel}' = 52$ G. For the restricted component, $S = 0.85$ and $2T_{\parallel}' = 63$ G.

As in virtually any spectral subtraction procedure, this one has some inherent subjectivity, but the procedure is validated by several key factors. The use of the no-ligand spectrum as one of the end points, i.e., a single component, may seem arbitrary, but it is justified by the shape of the spectrum,

Table I: Effects of Ligands on EPR Parameters of [^{2}H]-IASL SR[a]

sample	fraction	A/B	C/B
control	0	0.60 ± 0.01	0.37 ± 0.02
calcium	0.00 ± 0.05	0.60 ± 0.02	0.39 ± 0.06
AMPPNP	0.33 ± 0.01	0.65 ± 0.04	0.62 ± 0.01
AMPPNP/Ca	0.46 ± 0.01	0.69 ± 0.01	0.74 ± 0.03
ADP	0.21 ± 0.01	0.68 ± 0.01	0.50 ± 0.01
ADP/Ca	0.33 ± 0.03	0.66 ± 0.04	0.54 ± 0.01
ADP/Ca/P_i	0.27 ± 0.05	0.64 ± 0.02	0.50 ± 0.03
ADP/P_i	0.25 ± 0.05	0.67 ± 0.01	0.48 ± 0.03
MV_i	0.44 ± 0.04	0.66 ± 0.01	0.74 ± 0.04
DV_i	0.50 ± 0.03	0.61 ± 0.01	0.78 ± 0.04
P_i	0.00 ± 0.05	0.61 ± 0.01	0.32 ± 0.02

[a] Spectra were recorded at 4 °C in SRB. Ligands were added to the following concentrations: Ca, 0.45 mM; AMPPNP, 5 mM; ADP, 5 mM; P_i, 5 mM; MV_i, 5 mM; DV_i, 5 mM. Fraction represents the mole fraction in the restricted state (63 G). A/B and C/B are the ratios of the line heights illustrated in Figure 2. Spectral subtractions were performed as in the Methods and Spectral Subtraction sections. Errors are the standard error of the mean.

Table II: Dependence of Phosphate Effects on pH and DMSO[a]

sample	fraction	A/B	C/B
pH 6.0	0	1.05 ± 0.01	0.57 ± 0.03
pH 6.0, P_i	0.00 ± 0.05	1.12 ± 0.01	0.69 ± 0.04
pH 6.0, DMSO	0.80 ± 0.05	0.36 ± 0.01	0.54 ± 0.03
pH 6.0 DMSO/P_i	1.00 ± 0.05	0.45 ± 0.01	0.95 ± 0.05

[a] Spectra were recorded at 4 °C in 30 mM MES, 10 mM $MgCl_2$, 2 mM EGTA at pH 6.0. Inorganic phosphate (P_i) was added to 5 mM; DMSO was added to 40%. Fraction represents the mole fraction in the restricted state (63 G). A/B and C/B are the ratios of the line heights illustrated in Figure 2. Spectral subtractions were performed as in the Methods and Spectral Subtraction sections. Errors are the standard error of the mean.

which has little or no indication of spectral inhomogeneity. In particular, this spectrum clearly contains little or no contribution from the restricted component that is induced by ligand addition. The use of this mobile end point is further validated by the consistent restricted end-point spectrum obtained. In any event, even if we relax the assumption that the no-ligand spectrum corresponds to a single conformation, none of the key results of this study would be changed significantly. Regardless of the end points chosen, it remains clear that each ligand-induced spectrum can be constructed from a single pair of component spectra, strongly suggesting that the principal changes occurring are changes in discrete conformational populations.

Effect of Vanadate and Inorganic Phosphate. Mono- and decavanadate both broadened the EPR spectrum. As seen in Table I, the vanadates promote the formation of an additional component, characterized by the increase in A/B for monovanadate and in C/B for both mono- and decavanadate. Monovanadate addition resulted in a restricted mole fraction (f_R) of 44% (see Table I). Decavanadate addition resulted in an f_R of 50%. The results obtained here were observed within 10 min. An incubation for 24 h did not change the values of the spectral parameters.

The results obtained for the phosphoenzyme (E_2-P) differ from those obtained for vanadate. Experiments were performed in 30 mM MES, 10 mM $MgCl_2$, and 2 mM EGTA with and without 40% DMSO. These conditions were previously shown to promote maximal phosphoenzyme formation from inorganic phosphate (Lewis & Thomas, 1991). Table II indicates that the phosphoenzyme buffers alone had a substantial effect on the EPR spectrum. Compared to pH 7.4, the spectral parameters for the pH 6.0 buffers suggest decreased protein mobility but no resolvable component. With

Table III. Effects of Ca-ATPase Cycling on EPR Parameters[a]

sample	fraction	*A/B*	*C/B*
control		0.62 ± 0.02	0.46 ± 0.02
cycling	0.38 ± 0.04	0.66 ± 0.02	0.72 ± 0.03
final	0.23 ± 0.02	0.64 ± 0.01	0.53 ● 0.02

[a] Spectra were recorded at 4 °C in SRB with 30 mM imidazole, pH 7.4, 0.45 mM $CaCl_2$, 1 μg of A23187/0.05 mg of SR protein, 50 mM creatine phosphate, and a 20-fold excess of creatine kinase activity over the Ca-ATPase activity. Fraction represents the mole fraction in the restricted state (63 G). *A/B* and *C/B* are the ratios of the line heights illustrated in Figure 2. Spectral subtractions were performed as in the Methods and Spectral Substraction sections. Errors are the standard error of the mean.

DMSO addition, a restricted component could be resolved. By spectral subtractions, it was found that 80% of the protein was in a restricted conformation. This restricted conformation is not the same as that obtained at pH 7.4. The line widths are substantially broader for the DMSO-induced component.

Phosphoenzyme levels for IASL-labeled Ca-ATPase at 4 °C are 0.19 ± 0.07 and 0.24 ± 0.06 in 30 mM MES, 10 mM $MgCl_2$, and 2 mM EGTA with and without 40% DMSO, respectively. Labeling with IASL did not affect phosphoenzyme formation. The formation of the phosphoenzyme had no significant effect on the spectrum obtained in the absence of DMSO, as shown by the spectral parameters and the subtractions (see Table II). However, in the presence of DMSO the addition of phosphate broadened the spectrum and removed the remaining mobile component, making the transition from 80% to 100% restricted conformation complete. These results indicate that phosphoenzyme formation may have a small effect on protein mobility, but this effect is probably not relevant, since it is only observed in DMSO-containing solutions.

Effect of Calcium and Nucleotides Including Steady-State Calcium Transport. The addition of nucleotides promoted the formation of a second component, as evidenced by the increase in *A/B* and *C/B* (see Table I). These changes were seen for AMPPNP, AMPPNP/Ca, ADP, ADP/Ca, ADP/Ca/P_i, and ADP/P_i. Calcium had no effect at micromolar to millimolar concentrations; but it enhanced the effects of AMPPNP and ADP. The addition of mono- and decavanadate to ADP/Ca spectra produced results identical to vanadate alone.

Spectral subtractions clarify and quantitate these results. AMPPNP promoted an f_R of 33%, with an increase to 46% with micromolar calcium. ADP promoted an f_R of 21%, with an increase to 33% with micromolar calcium. The addition of P_i decreased this fraction to 25% (identical to ADP/P_i). The f_R reached for ADP plus calcium and vanadate was identical to that obtained for the vanadate alone. The subtractions also illustrate which combinations of ligands promote identical fractions of the two conformations (ADP and ADP/Ca/P_i and ADP/P_i; AMPPNP and ADP/Ca), see Table I.

Qualitatively similar results were obtained at 25 °C, but spectral subtractions were not possible because the field positions for the two components were too similar, preventing adequate spectral resolution.

The IASL-labeled Ca-ATPase was studied under conditions of steady-state Ca-dependent ATP hydrolysis (see Table III). The addition of ATP to the sample increased *A/B* and especially *C/B*. These changes are consistent with a restriction in protein mobility. Following ATP hydrolysis, the spectral parameters reversed to values consistent with the hydrolysis products of ADP, calcium, and phosphate, which broadened

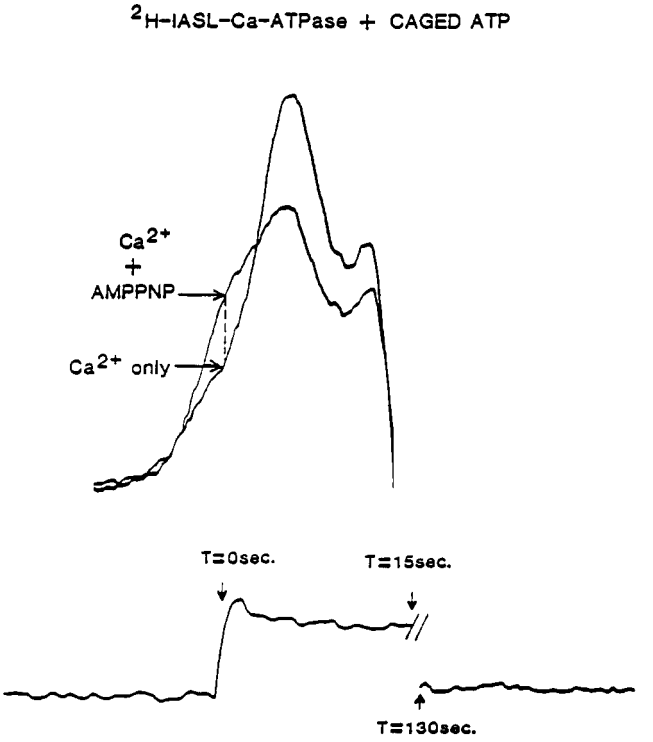

FIGURE 4: Photolysis of caged ATP. Spectra were recorded at 4 °C in SRB with the addition of 20 mM imidazole, pH 7.4, 0.45 mM $CaCl_2$, 1 μg of A23187/0.05 mg of SR protein, and 5 mM caged ATP. Protein concentration was 20 mg/mL. The spectrum was monitored at the indicated field position (vertical dashed line). The lower trace indicates the intensity of this position versus time (at 2× gain). At the indicated position ($T = 0$) ATP was released by light.

the spectrum in the same way. Based on the subtractions, the cycling enzyme has an f_R of 38%, whereas the final spectrum (after ATP depletion) has a value of 23%. This final value is not significantly different from the fraction obtained for ADP/Ca/P_i. This conformation is essentially identical to the restricted components found in the vanadate and nucleotide studies. It should be noted that the maximum value obtained with ATP and calcium is less than the value of AMPPNP and calcium. This suggests that a fraction of the enzyme is in an intermediate state that is not characterized by a restricted conformation. A likely candidate (under the experimental conditions) is the E_2-P state.

ATP is immediately hydrolyzed upon binding in the presence of calcium. Therefore, an $E_1 \cdot Ca_2$·nucleotide state is not predicted for ATP and calcium. The conditions used to induce steady-state transport of calcium would result in E_1-P·Ca_2 being the predominant state (Shigekawa et al., 1978). This implies that the E_1-P·Ca_2 state contains a restricted conformation.

Transient Calcium Transport Using Caged ATP. The time resolution produced by photolysis of caged ATP should help resolve the ATPase cycle in time, thus clarifying the correlation of conformational and biochemical events. Figure 4 shows the results obtained under transient conditions. Using caged ATP, the promotion of the restricted component could be recorded immediately upon ATP formation. The spectrum was monitored at the indicated field position (corresponding to *C*) versus time. The signal at this field position increases with the formation of the restricted conformation. At the indicated time, light released the ATP (1–1.5 mM). The intensity increased, decayed to a steady-state, and returned to a baseline in approximately 2 min. This was quantitated as the percent increase in the line height of *C*. The increase

was about 40% compared to the control. AMPPNP and calcium addition resulted in an increase of 75%. This is consistent with the steady-state findings that ATP does not cause as large a change as AMPPNP. The spectrum following ATP hydrolysis was identical to the control except for spectral changes consistent with ADP, calcium, and phosphate.

A transient overshoot was observed in the intensity at the monitored spectral position. This suggests that there is a buildup of the restricted conformation before steady-state conditions are reached, in which the restricted conformation becomes less populated than during the transient phase. This may reflect the rate-limiting step referred to above.

DISCUSSION

Summary of Results. The calcium transport cycle of the sarcoplasmic reticulum Ca-ATPase is postulated to involve transitions between two or more distinct conformational states. Transitions during the cycle would occur when the relative thermodynamic stabilities of these states were changed by substrate binding, ATP hydrolysis, phosphorylation, and dephosphorylation (Jencks, 1982; Eisenberg & Hill, 1985). Using EPR spectroscopy, we have studied the effects of substrates on the nanosecond rotational dynamics of the Ca-ATPase. Changes in this time range reflect changes in internal protein dynamics and, therefore, changes in enzyme conformation.

In the absence of specific ligands, the EPR spectrum of IASL-labeled Ca-ATPase is consistent with a single motional state of the probe (except for a more mobile population that accounts for no more than 5% of the spin labels), but the addition of nucleotides or vanadate produces spectra containing at least two components (Figure 2). By using perdeuterated IASL, we obtained sufficient resolution to show, by spectral subtraction, that these spectra appear to consist of two distinct components, one identical to the no-ligand control spectrum and the other more restricted in rotational mobility. Calcium alone has no effect but enhances the effects of nucleotides. When AMPPNP/Ca, monovanadate, or decavanadate was present, the restricted component represented approximately 50% of the spectrum. A lower percentage was present with ligands such as ADP, ADP/Ca, AMPPNP, ATP, or ATP/Ca. The formation of the phosphoenzyme by inorganic phosphate did not induce this component, except possibly in the presence of DMSO. By using flash photolysis of caged ATP, we obtained time-resolved EPR signals during the Ca-ATPase cycle, showing that the population of the restricted component undergoes biphasic changes during the transient phase of ATP hydrolysis in the presence of calcium.

Distinct Conformational States. In comparison to the control spectrum, the ligands that affected the spectrum caused a restriction in probe rotational mobility. Although different ligands affected the spectra to different extents, the *end-point* spectrum, obtained after subtracting the control spectrum until a valid single-component spectrum was obtained, was essentially invariant at 4 °C and pH 7.4 in aqueous medium. The same two components were observed during the steady state of the active enzyme cycle. Thus this protein-bound spin label appears to resolve two distinct dynamic states, regardless of the combination of ligands bound to the protein. One of these states is predominant in the resting enzyme (no ligands), and the other is induced by certain ligands. The spectrum for the resting conformation has a splitting of 52 G and an effective order parameter of 0.53. The spectrum for the added conformation has a splitting of 63 G and an order parameter of 0.85 (much more restricted). Although differences in the rate and amplitude of rotational motion are the most likely explanations for the differences between these two components, minor contributions from other effects, such as environmental polarity, cannot be ruled out. Nevertheless, the presence of other effects would in no way invalidate the observation of two apparent conformational states detected by the spin label.

Despite the addition of saturating concentrations of ligands, a spectrum corresponding only to the restricted conformation (f_R = 1) was not achieved under any of the physiological conditions studied, indicating that the ligands perturb the equilibrium (or steady-state) distribution between the two states but that there is not a one-to-one correspondence between ligand binding and conformational change. That is, *the apparent equilibrium constant for the transition between the two conformations is finite*, even in the presence of saturating concentrations of some ligands. This result is reminiscent of the observation that the conformational equilibrium for spin-labeled myosin is shifted by ATP binding but that both conformations coexist even in the presence of saturating ATP (Barnett & Thomas, 1987). Of course, there may be more than two conformational states present in the spin-labeled Ca-ATPase, but if so, they are not resolved in the EPR spectrum.

Other explanations for the two resolved spectral components are possible but unlikely. The spectral changes could arise from a label bound to two sites of equal reactivity, one sensitive to ligands, the other not. However, iodoacetamide labels have been shown to be quite specific for a single site on the Ca-ATPase, Cys-674 (Yamashita & Kawakita, 1987; Suzuki et al., 1987; Birmachu et al., 1989), and previous observations on IASL-labeled SR support the observation of spectral heterogeneity despite single-site labeling (Coan & Keating, 1982; Coan, 1983). Another artifactual source of spectral heterogeneity would be a large fraction (about half) of the labeled enzymes that are inactive and insensitive to ligand binding. However, in the presence of DMSO and P_i at pH 6.0, the labeled protein attained a fully restricted conformation (f_R = 1, Table II), suggesting that at least with DMSO the equilibrium between the two conformations is shifted entirely toward the restricted state. Thus, while multiple labeling sites or an inactive enzyme population cannot be ruled out entirely, these are probably not the source of the two spectral components and the observed changes. A direct steric interaction between the nucleotide site and the spin label is unlikely, since previous work has shown that the iodoacetamide binding site (using IAEDANS) is at least 50 Å from the nucleotide site (Squier et al., 1987; Birmachu et al., 1989). Of course, the resolution of two motional states of a site-specific spin label does not imply that this conformational transition is evident throughout the protein's structure. However, the conformational transitions we are detecting are being propagated over long distances through the protein and are thus likely to provide insight into the energy transduction process in the Ca-ATPase.

Relationship to the Ca-ATPase Kinetic Cycle. The relationship of the present work to the widely discussed kinetic model is illustrated by Scheme II, in which boxes indicate those ligand states in which a significant fraction of the restricted conformation (f_R) is detected by the EPR spectra. In contrast to results from several fluorescence studies (discussed in the introduction), this spin label does not detect the binding of Ca^{2+} to the high-affinity binding sites (Table I). Our results on other ligand effects (Table I) are quite consistent with previously reported findings using IASL–Ca-ATPase (Coan et al., 1979, 1986; Coan & Keating, 1982;

Scheme II: Proposed Ca-ATPase Kinetic Cycle[a]

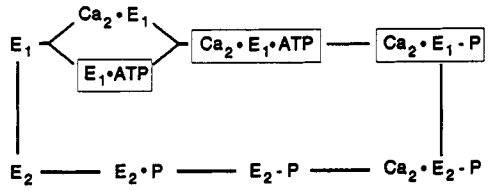

[a] The rectangles enclose the states that have significant populations of the restricted component.

Coan, 1983), although the use of deuterated IASL in the present study permits resolution of the discrete spectral components. We confirm that nucleotides increase spin-label restriction and that this effect is enhanced by Ca^{2+} (Table I). We have also confirmed and further quantitated the effects of vanadate, which clearly increases f_R (Table I). Since vanadate has been proposed to act as a high-affinity phosphate analog in inhibiting the Ca-ATPase (O'Neal et al., 1979; Dupont & Bennett, 1982; Ortiz et al., 1984; Varga et al., 1985), this might be taken as evidence that E_2-P has increased f_R (Coan et al., 1986). However, we find that the phosphoenzyme formed by the addition of P_i at pH 6.0 does not have an elevated f_R (Table I). Since this complex, rather than that produced by vanadate, is more likely to correspond to the E_2-P state depicted in Scheme II, we conclude that E_2-P does not have a significant population of the restricted component detected by IASL. *Thus vanadate does not appear to mimic phosphate faithfully in this system*; its effects on protein conformation, as detected by IASL, are more like those of nucleotides than those of phosphate.

Previous studies have shown that DMSO increases phosphorylation from inorganic phosphate, presumably by decreasing the water concentration and thus favoring phosphoenzyme formation and stabilizing the phosphoenzyme from hydrolysis (de Meis et al., 1982). The presence of 40% DMSO does result in a slight effect of subsequent P_i addition on f_R (Table II), consistent with the results of Coan (1983). As indicated above, since this does not agree with the effects of phosphoenzyme formation in the absence of DMSO ($f_R = 0$ Table I), the most straightforward explanation is that the conformational states produced in the presence of DMSO do not correspond to the normal intermediates in the cycle. This conclusion is supported by the observations that (a) DMSO has a large effect on the spectrum even in the absence of P_i (Table II), producing spectral changes that are qualitatively different from those of other ligands, (b) the effects of DMSO on calcium uptake by SR are only partially reversible (The & Hasselbach, 1977), and (c) DMSO by itself has been shown to cause large-scale aggregation of the Ca-ATPase in the SR membrane (Squier & Thomas, 1988).

During steady-state calcium-dependent ATP hydrolysis, both the mobile and restricted conformations are present (Table I). This suggests that the formation of $Ca_2 \cdot E_1$-P, which should be predominant under these conditions (Shigekawa & Dougherty, 1978a,b; Shigekawa et al., 1978), stabilizes the restricted conformation. However, since ADP also increases f_R (Tables I and II), it is important to obtain EPR signals during the early phase of the ATPase reaction, before ADP has had time to accumulate. The transient EPR studies with caged ATP (Figure 4) provide this information. The rapid rise in the EPR signal intensity during the transient phase probably indicates an increase in f_R, although further studies at other spectral positions would be required to rule out the production of a new (third) spectral component. Our results indicate a transient overshoot in the amount of restricted conformation induced, before the intermediate steady-state level is reached. This overshoot probably reflects a *pre-steady-state conformational change in the transport cycle corresponding to a transient increase in the population of the proposed $Ca_2 \cdot E_1$-P state*, followed by a decline as the *$Ca_2 \cdot E_2$-P* and E_2-P states, which must have a lower value of f_R, are produced. This interpretation is supported by the finding that the transition between these two phosphoenzyme states is rate-limiting under these conditions (Shigekawa & Dougherty, 1978), and by previous studies on phosphoenzyme levels in a calcium-preincubated enzyme, which have shown a transient overshoot upon ATP addition (Froehlich & Taylor, 1976; Stahl & Jencks, 1987). Therefore, the most straightforward interpretation is that $Ca_2 \cdot E_1$-P has an elevated f_R, while $Ca_2 \cdot E_2$-P and/or E_2-P do not. This is consistent with our observation that E_2-P formation from P_i does not elevate f_R (Table I).

Comparison with Transient EPR Measurements of Global Dynamics. The present study is complementary to analogous work done with a maleimide spin label (MSL) that is sensitive mainly to microsecond (global) dynamics (Lewis & Thomas, 1991). As in the present study, a wide range of ligand conditions were tested, including transient ATP hydrolysis induced by photolysis of caged ATP. In contrast to the substantial changes in nanosecond motions detected by IASL, no changes in global dynamics were observed as a function of nucleotides and other ligands, including measurements during the ATPase cycle. Fluorescence energy transfer and FTIR studies have also failed to show evidence for large-scale ligand-induced structural changes in the Ca-ATPase (Birmachu et al., 1989; Martonosi et al., 1990; Jona et al., 1990). This tends to rule out large-scale shape changes and changes in oligomeric state (protein–protein interactions) and supports the conclusion that the changes detected in the present study correspond to transitions in internal dynamics that are propagated through the protein's structure.

Conclusion. Using perdeuterated IASL, we have obtained direct evidence for (at least) two resolved conformational states within the Ca-ATPase, as distinguished by nanosecond mobility of the spin label. We conclude that the Ca-ATPase can exist in at least two internal conformations whose relative populations are affected by substrate ligands. Both conformations are present in substantial amounts in the following proposed states: $E_1 \cdot ATP$, $Ca_2 \cdot E_1 \cdot ATP$, and $Ca_2 \cdot E_1 \cdot P \cdot Ca_2$. The resting enzyme ($E_1$ and E_2), $Ca_2 \cdot E_1$, and E_2-P do not have significant populations in the restricted conformation. Thus, the conformational changes found in this study do not correspond simply to the proposed E_1 to E_2 transition. The use of caged ATP has permitted the first transient EPR studies on this system, providing more direct insight into the conformational transitions occurring in the Ca-ATPase cycle. In the future this work should be extended to a more detailed study of the transient kinetics of the Ca-ATPase cycle. By use of caged ATP, caged P_i, and caged Ca^{2+}, the conformations can be monitored as a function of time and transport conditions, so that the biochemical kinetics of the calcium transport cycle can be correlated directly with the dynamic physical states of the protein.

ACKNOWLEDGMENT

We thank Albert H. Beth and Yale Goldman for their generous gifts of the perdeuterated spin label and caged ATP, respectively. We thank James E. Mahaney for helpful discussions and for assistance with the phosphoenzyme measurements. We thank Robert L. H. Bennett for technical assistance and computer programming.

REFERENCES

Arrondo, J. L. R., Mantsch, H. H., Mullner, N., Pikula, S., & Martonosi, A. (1987) *J. Biol. Chem. 262*, 9037.

Barnett, V. A., & Thomas, D. D. (1987) *Biochemistry 26*, 314.

Barrabin, H., Scofano, H. M., & Inesi, G. (1984) *Biochemistry 23*, 1542.

Bigelow, D. J., Squier, T. C., & Thomas, D. D. (1986) *Biochemistry 25*, 194.

Birmachu, W., Nisswandt, F., & Thomas, D. D. (1989) *Biochemistry 28*, 3940.

Blasie, J., Pascolini, D., Asturias, F., Herbette, L., Pierce, D., & Scarpa, A. (1990) *Biophys. J. 58*, 687.

Brandl, C. J., Green, N. M., Korczak, B., & MacLennan, D. H. (1986) *Cell 44*, 597.

Chen, P. S., Toribara, T. Y., & Warner, H. (1956) *Anal. Chem. 28*, 1756.

Coan, C. (1983) *Biochemistry 22*, 5826.

Coan, C. R., & Inesi, G. (1977) *J. Biol. Chem. 252*, 3044.

Coan, C., & Keating, S. (1982) *Biochemistry 21*, 3214.

Coan, C., Verjovski-Almeida, S., & Inesi, G. (1979) *J. Biol. Chem. 254*, 2968.

Coan, C., Scales, D. J., & Murphy, A. J. (1986) *J. Biol. Chem. 261*, 10394.

de Meis, L., de Souza Otero, A., Martins, O. B., Alves, E. W., Inesi, G., & Nakamoto, R. (1982) *J. Biol. Chem. 257*, 4993.

Dupont, Y., & Leigh, J. (1978) *Nature 273*, 396.

Dupont, Y., & Bennett, N. (1982) *FEBS Lett. 139*, 237.

Dux, L., & Martonosi, A. (1983a) *J. Biol. Chem. 258*, 2599.

Dux, L., & Martonosi, A. (1983b) *J. Biol. Chem. 258*, 10111.

Eisenberg, E., & Hill, T. L. (1985) *Science 227*, 999.

Fajer, P. G., Fajer, E. A., Matta, J. J., & Thomas, D. D. (1990) *Biochemistry 29*, 5865.

Fernandez, J. L., Rosemblatt, M., & Hidalgo, C. (1980) *Biochim. Biophys. Acta 599*, 552.

Freed, J. (1976) in *Spin Labeling—Theory and Applications* (Berliner, K. J., Ed.) pp 53–132, Academic Press, New York.

Froehlich, J., & Taylor, E. (1976) *J. Biol. Chem. 251*, 2307.

Gaffney, B. J. (1976) in *Spin Labeling—Theory and Applications* (Berliner, L. J., Ed.) pp 567–571, Academic Press, New York.

Girardet, J., & Dupont, Y. (1992) *FEBS Lett. 296*, 103.

Gornall, A. G., Bardawill, C. J., & David, M. M. (1949) *J. Biol. Chem. 177*, 751.

Herbette, L., Scarpa, A., Blasie, J. K., Bauer, D. R., Wang, C. T., & Fleischer, S. (1981) *Biophys. J. 36*, 27.

Hidalgo, C., Thomas, D. D., & Ikemoto, N. (1978) *J. Biol. Chem. 253*, 6879.

Ikemoto, N., Morgan, T., & Yamada, S. (1978) *J. Biol. Chem. 253*, 8027.

Inesi, G., Sumbilla, C., & Kirtley, M. E. (1990) *Physiol. Rev. 70*, 749.

Jencks, W. (1982) in *Membranes and Transport* (Martonosi, A. N., Ed.) Vol. I, pp 515–526, Plenum Press, New York.

Jencks, W. P. (1989) *J. Biol. Chem. 264*, 18855.

Jona, I., Matko, J., & Martonosi, A. (1990) *Biochim. Biophys. Acta 1029*, 183.

Jost, P. C., & Griffith, O. H. (1978) in *Biomolecular Structure and Function* (Agris, P. F., Ed.) pp 25–54, Academic Press, New York.

Kaplan, J. H., Forbush, B., III, & Hoffman, J. F. (1978) *Biochemistry 17*, 1929.

Kubo, K., Suzuki, H., & Kanazawa, T. (1990) *Biochim. Biophys. Acta 1040*, 251.

Laggner, P., Suko, J., Punzengruber, C., & Prager, R. (1981) *Z. Naturforsch. 36B*, 1136.

Lanzetta, P. A., Alvarez, L. J., Reinsch, P. S., & Candia, O. A. (1979) *Anal. Biochem. 100*, 95.

Lewis, S. M., & Thomas, D. D. (1986) *Biochemistry 25*, 4615.

Lewis, S. M., & Thomas, D. D. (1991) *Biochemistry 30*, 8331.

Martonosi, A. N., Jona, I., Molnar, E., Seidler, N. W., Buchet, R., & Varga, S. (1990) *FEBS Lett. 268*, 365.

McCray, J. A., Herbette, L., Kihara, T., & Trentham, D. R. (1980) *Proc. Natl. Acad. Sci. U.S.A. 77*, 7237.

Murphy, A. (1978) *J. Biol. Chem. 253*, 385.

O'Neal, S. G., Rhoads, D. B., & Racker, E. (1979) *Biochem. Biophys. Res. Commun. 89*, 845.

Ortiz, A., Garcia-Carmona, F., Garcia-Canovas, F., & Gomez-Fernandez, J. (1984) *Biochem. J. 221*, 213.

Petithory, J. R., & Jencks, W. P. (1986) *Biochemistry 25*, 4493.

Pick, U., & Karlish, S. (1980) *Biochim. Biophys. Acta 626*, 255.

Pick, U., & Karlish, S. (1982) *J. Biol. Chem. 257*, 6120.

Shigekawa, M., & Dougherty, J. P. (1978a) *J. Biol. Chem. 253*, 1451.

Shigekawa, M., & Dougherty, J. P. (1978b) *J. Biol. Chem. 253*, 1458.

Shigekawa, M., Dougherty, J. P., & Katz, A. M. (1978) *J. Biol. Chem. 253*, 1442.

Squier, T. C., & Thomas, D. D. (1986a) *Biophys. J. 49*, 921.

Squier, T. C., & Thomas, D. D. (1986b) *Biophys. J. 49*, 936.

Squier, T. C., & Thomas, D. D. (1988) *Biol. Chem. 263*, 9171.

Squier, T. C., Bigelow, D. J., deAncos, J. G., & Inesi, G. (1987) *J. Biol. Chem. 262*, 4748.

Squier, T. C., Hughes, S. E., & Thomas, D. D. (1988) *J. Biol. Chem. 263*, 9162.

Stahl, N., & Jencks, W. P. (1987) *Biochemistry 26*, 7654.

Sumida, M., Wang, T., Mandel, F., Froehlich, J., & Schwartz, A. (1978) *J. Biol. Chem. 253*, 8772.

Suzuki, H., Obara, M., Kuwayama, H., & Kanazawa, T. (1987) *J. Biol. Chem. 262*, 15448.

The, R., & Hasselbach, W. (1977) *Eur. J. Biochem. 74*, 611.

Thomas, D. D., & Hidalgo, C. (1978) *Proc. Natl. Acad. Sci. U.S.A. 75*, 5488.

Varga, S., Csermely, P., & Martonosi, A. (1985) *Eur. J. Biochem. 148*, 119.

Vilsen, B., & Andersen, J. P. (1987) *Biochim. Biophys. Acta 898*, 313.

Watanabe, T., & Inesi, G. (1982a) *Biochemistry 21*, 3254.

Watanabe, T., & Inesi, G. (1982b) *J. Biol. Chem. 257*, 11510.

Yamashita, T., & Kanakita, M. (1987) *J. Biochem. 101*, 377.

Yasouka-Yabe, K., & Kawakita, M. (1983) *J. Biochem. 94*, 665.

Yasouka-Yabe, K., Tsuji, A., & Kawakita, M. (1983) *J. Biochem. 94*, 677.